

RESEARCH ARTICLE

Broadband Circularly Polarized Antenna Array via Metasurface and Partially Emptied Substrate

FRANCESCO ANELLI¹, ANTONELLA MARIA LOCONSOLE¹, RICCARDO LOSITO,
AND FRANCESCO PRUDENZANO¹, (Member, IEEE)

Department of Electrical and Information Engineering, Politecnico di Bari, 70125 Bari, Italy

Corresponding author: Francesco Prudenzano (francesco.prudenzano@poliba.it)

This work was supported in part by the Agenzia Spaziale Italiana (ASI) 2024-68-I.0 “Origami Reconfigurable Beam-steering Antennas with METAsurfaces for Communication on Small Satellites-ORBIT-META” under Grant CUP: F93C24000550001; in part by the Ministero dell’Istruzione e del Merito (MIUR) Progetti di Rilevante Interesse Nazionale (PRIN) 2022, Italian National Recovery and Resilience Plan (NRPP)–DD n. 1181 del 27-07-2023-Innovative Technologies for non-invasive assessment of plant health condition to support precision farming “VEGETATION” under Grant P2022ZF9P2 and Grant CUP: I53D23005710 001; in part by the European Union under NRRP of NextGenerationEU, with reference to the partnership on “Telecommunications of the Future” (Program “RESTART”) through the Structural Project Antennas and Devices for mixing, detection and manipulation of mmWaves under Grant PE00000001 and Grant CUP: D93C22000910001; in part by ASI 687/2022-Ministero dell’Università e della Ricerca (MUR) 341 15/03/22 “SPACE IT UP” under Grant CUP: D53C24000570006; and in part by HORIZON-Training Mobility Actions (TMA)-Marie Skłodowska-Curie Actions (MSCA)-Staff Exchanges (SEs) HORIZON TMA MSCA SEs “Cr4+:YAG/Polymer Nanocomposite as Alternative Materials for Q-Switched Lasers: Properties, Modeling, and Applications—ALTER-Q” under Grant 101182995.

ABSTRACT A metasurface including an empty region constituted by a square-shaped aperture is proposed to improve the performance of a circularly polarized patch antenna array based on sequential-phase feeding. The metasurface is applied/stacked to a conventional antenna consisting of a loop feeding structure, which enables sequential incremental phase to four patches. Surface waves propagating on the metasurface are excited, affecting the resonance features of the overall radiating structure, thereby improving both the input impedance-matching and the axial ratio bandwidths of the antenna. The square-shaped aperture in the top layer is introduced to extend the range of frequency over which the sequential phase feeding remains effective. The antenna prototype and the stacked metasurface are fabricated. The experimental results, in good agreement with simulation, show that the antenna with the compact size $2.16\lambda_0 \times 2.16\lambda_0 \times 0.12\lambda_0$, at the central frequency, provides a broad impedance relative bandwidth of 43.8% from 11.6 GHz to 18.1 GHz and a 3-dB axial ratio bandwidth of 36.6% (from 11.6 GHz to 16.8 GHz). In addition, the proposed antenna has a flat gain within the operating frequency band and a peak gain $G = 13.9$ dBic at frequency $f = 14$ GHz.

INDEX TERMS Axial ratio, circular polarization, metasurface, patch antenna, satellite communications, sequential-phase, wideband antenna.

I. INTRODUCTION

Microstrip patch antennas are widely employed to address the demands of modern communication, which usually include wideband operation, high efficiency, ease of fabrication, and low manufacturing costs [1]. These antennas are crucial for applications such as satellite communication and global positioning systems (GPS), where circular polarization (CP) is required to ensure reliable signal transmission and reception [2]. CP radiation offers several advantages,

The associate editor coordinating the review of this manuscript and approving it for publication was Ravi Kumar Gangwar¹.

including enhanced immunity to multipath fading, reduced polarization mismatch losses, and mitigation of Faraday rotation effects caused by the ionosphere [3]. Among several antenna structures for generating CP, single-feed designs have been widely investigated allowing compact radiating structures and simplicity in design [4]. However, these antennas generally suffer from narrow impedance matching and axial ratio (AR) bandwidths, which limit their performance across wide frequency ranges [5]. To overcome these limitations, several bandwidth enhancement techniques have been proposed, including the use of parasitic patches, slotted ground planes, and resonant structures [6], [7], [8], [9], [10].

Among the feeding networks, the sequential-phase technique has gained significant attention due to its capability of improving both the impedance and *AR* bandwidths. Therefore, sequential-phase feeding constitutes a promising and feasible approach for broadband CP antenna arrays [11], [12]. Additionally, the integration of metasurfaces, either above or below the radiating element, with or without an air gap, has demonstrated a strong potential in further enhancing antenna performance by handling surface wave propagation and improving radiation characteristics [3], [13].

In particular, the Ku-band (12 – 18 GHz) is of growing importance for high-data-rate satellite communications, direct broadcast services, and radar systems, necessitating antenna designs that combine compact form factors with broad CP bandwidth and stable performance.

In this paper, we present the use of a metasurface including a square-shaped aperture as a method to enhance the performance of a circularly polarized sequential-phase-fed array. The metasurface aperture is positioned above the feeding network, to reduce the phase-dispersion across frequencies. This configuration, proposed for the first time to the best of our knowledge, operates by reducing the effective permittivity ϵ_{eff} of the microstrip lines, thereby decreasing phase-delay across frequencies. The resulting two-layer antenna achieves broadband CP operation across the Ku-band. We demonstrate that the employment of the square-shaped aperture significantly enhances the antenna overall performance, improving the impedance bandwidth from 9.7% to 43.8% and the *AR* bandwidth from 10% to 36.6%. Furthermore, the gain *G* as a function of frequency *f* remains stable within the impedance bandwidth, ensuring consistent performance throughout the Ku-band. The proposed method provides an effective solution for typical satellite communication systems requiring compact, high-performance, and broadband CP antennas.

II. DESIGN OF THE CP ANTENNA ARRAY

The proposed antenna configuration is composed of two substrates. Rogers RT/duroid 5880 substrates ($\epsilon = 2.2$, $\tan\delta = 0.0009$) are considered for both layers. Figure 1 (a) illustrates the top side of substrate #1 with thickness $h_1 = 0.787$ mm. This array follows the design approach similar to that presented in [14], optimized for CP and broadband performance. The bottom side of substrate #1 is fully metalized, serving as a ground plane. Figure 1 (b) illustrates the top side of substrate #2 with thickness $h_2 = 1.575$ mm, which is stacked on the top layer of substrate #1 with no airgap, to increase the compactness. Substrate #2 is covered by copper on a single side. Sequential-phase feeding relies on delivering specific phase shifts to each element (0° , 90° , 180° , and 270° in the proposed antenna) to generate CP. However, the phase shifts are frequency-dependent, and higher dispersion is introduced when the feeding network is loaded with a dielectric, especially if characterized by high permittivity. To mitigate this, a square-shaped aperture is introduced above the sequential-phase feeding network.

This design choice reduces the variation in phase delay across frequencies by lowering the effective permittivity ϵ_{eff} . Specifically, the aperture reduces the effective permittivity of the microstrip lines in the loop feeding network from about $\epsilon_{eff}=2.14$ to $\epsilon_{eff} = 1.75$. Similarly, the microstrip lines used to feed the four patches exhibit a reduction in effective permittivity due to the aperture from about $\epsilon_{eff}=2.1$ to $\epsilon_{eff}=1.69$.

To evaluate the performance of the antenna, the entire structure is simulated using CST Microwave Studio. The optimized design parameters are summarized in Table 1. The metasurface, working as an artificial magnetic conductor (AMC), is directly stacked on the primary radiator. In particular, a 2×2 unit-cell pattern is stacked on each patch of the primary radiator in order to excite the suitable surface waves [15], [16], [17]. A cavity model can be employed to determine the surface wave resonance:

$$\beta_{SW} = \pi/NP \quad (1)$$

where β_{SW} is the propagation constant of the surface wave, $N = 0, 1, 2, \dots$, is the number of unit cells and $P = l_m + g_m$ is the unit cell periodicity [1], [17], [18].

Unit cell simulation via eigenmode solver in CST Microwave Studio has been employed to obtain the dispersion diagram, i.e. the eigenmode frequency as a function of the phase constant. Periodic boundaries have been applied to the side walls of the unit cell and electric conductor ($E_t = 0$) boundaries have been considered at the top and bottom, separated from the unit cell by an air gap. The dispersion diagram is presented in Fig. 2(a). Specifically, for a 2×2 -unit cell distribution, the first two eigenmodes, i.e. transverse magnetic (TM) and transverse electric (TE), exhibit the resonant frequencies $f_{r-TM} = 15.1$ GHz and $f_{r-TE} = 16.4$ GHz, respectively. These frequencies have been obtained by intersecting the dispersion curves of Fig. 2(a), with the value on the right side of (1) for $N = 2$ [15], [17].

Furthermore, Fig. 2(b) illustrates the reflection phase ρ , computed through unit-cell simulation in the frequency domain. Periodic boundaries have been applied to the side walls of the unit cell, Floquet port at the top of the unit cell, and electric conductor ($E_t = 0$) at the bottom of the unit cell. The results indicate that the entire Ku-band lies within the AMC bandwidth, which is defined as the frequency range where the reflection phase remains between $\rho = -90^\circ$ and $\rho = +90^\circ$ [19]. Therefore, in-phase reflections for an incident wave over a large bandwidth is obtained, this leading to efficient radiation also in case of adjacent substrates [17]. Moreover, also for oblique incidences, the AMC bandwidth is stable; this is crucial for array scanning stability radiation.

In order to further verify the achievement of CP, simulated surface current distributions at the frequency $f = 12$ GHz are illustrated in Fig. 3. It can be observed that the patch elements are excited along one diagonal of the array at a phase $\varphi = 0^\circ$ and along the orthogonal diagonal at $\varphi = 90^\circ$, with similar behaviour also at $\varphi = 180^\circ$ and $\varphi = 270^\circ$. The observed surface current distribution, with the vector rotating by 90° at successive 90° phase increments, confirms that the antenna

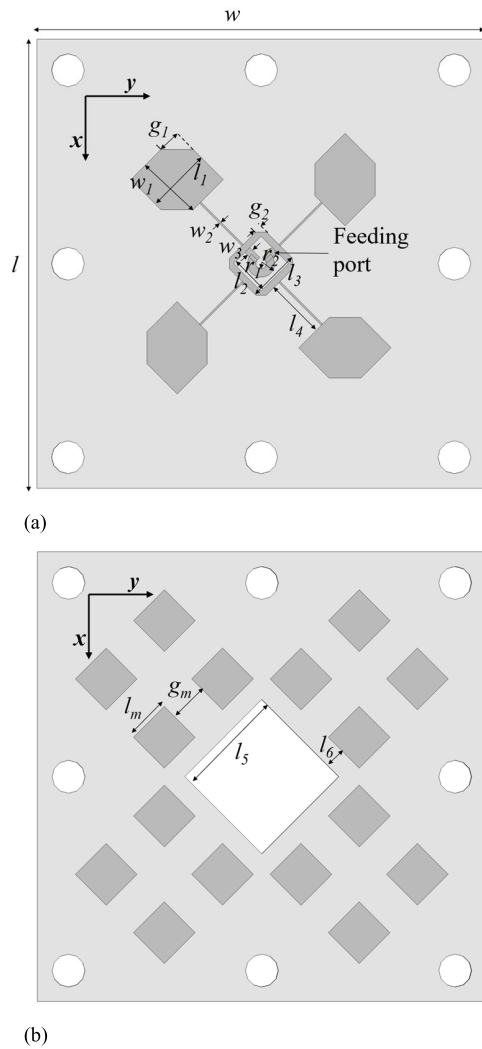


FIGURE 1. Geometry and size of the proposed 2×2 sequential phase-fed patch array with a stacked metasurface; (a) top side of substrate #1, (b) top side of substrate #2.

TABLE 1. Geometric dimensions of the optimized antenna.

Parameter	Value	Parameter	Value	Parameter	Value
g_1	2.2 mm	w	43.6 mm	l_2	3.77 mm
g_2	0.73 mm	r_1	0.505 mm	l_3	5.07 mm
g_m	3.76 mm	r_2	1.315 mm	l_4	5.84 mm
w_1	6.35 mm	l	43.6 mm	l_5	10.6 mm
w_2	0.17 mm	l_m	4.24 mm	l_6	1.98 mm
w_3	0.7 mm	l_1	6.35 mm		

supports CP. Similar current patterns were observed at other frequencies across the operational bandwidth, confirming consistent CP behavior, but are omitted here for brevity.

To investigate the influence of the square-shaped aperture positioned above the sequential-phase feeding network, a series of parametric simulations have been conducted by varying the l_5 value. Figure 4 (a) highlights a substantial improvement of the impedance bandwidth for $l_5 = 10.6$ mm (11.3 – 17.8 GHz) with respect to the case of no aperture,

i.e. $l_5 = 0$ mm. Figure 4 (b) illustrates the large 3 – dB AR bandwidth (11.4 – 18.2 GHz) for $l_5 = 10.6$ mm.

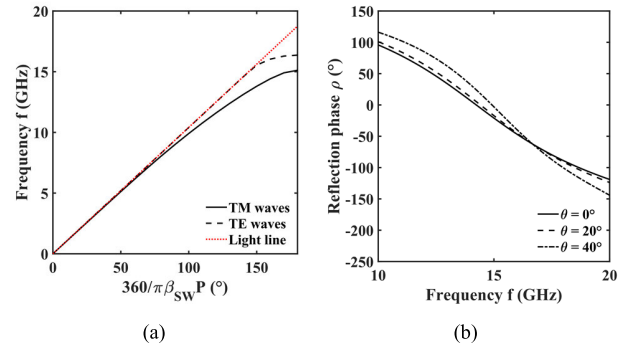


FIGURE 2. Simulated (a) dispersion diagram and (b) reflection phase ρ for different incidence angle θ of the metasurface structure.

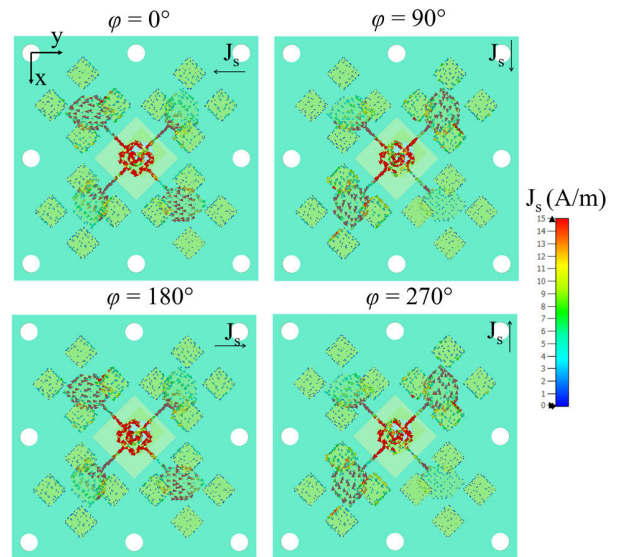


FIGURE 3. Surface current distribution for phase $\varphi = 0^\circ, \varphi = 90^\circ, \varphi = 180^\circ$ and $\varphi = 270^\circ$ at the frequency $f = 12$ GHz.

III. FABRICATION AND CHARACTERIZATION OF THE CP ANTENNA ARRAY

Prototypes of the antenna have been fabricated by using printed circuit board (PCB) process, via ultraviolet (UV) laser writing. Figure 5 (a) reports the top side of the bottom substrate, Fig. 5 (b) the top side of the top substrate and Fig. 5 (c) the mounted circularly polarized antenna inside the Satimo StarLab anechoic chamber. The input reflection coefficient S_{11} has been measured with the Agilent Technologies N5224A PNA Network Analyzer, while the radiation performance by the abovementioned Satimo StarLab anechoic chamber operating up to the frequency $f = 18$ GHz.

Figure 6 (a) reports the simulated (solid line) and measured (dashed line) input reflection coefficient S_{11} . The measured impedance bandwidth covers from $f = 11.6$ GHz to $f = 18.1$ GHz, i.e. the relative bandwidth is 43.8%. A very good agreement between simulation and measurement is obtained. The slight discrepancies could be due

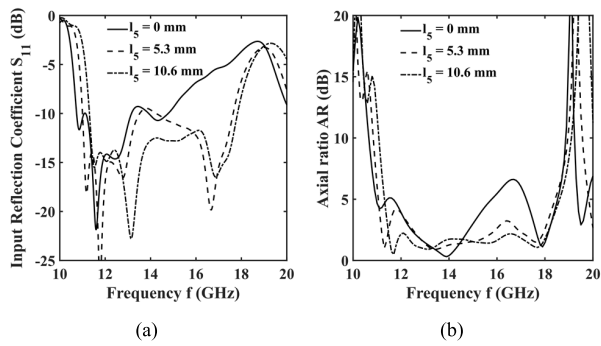


FIGURE 4. Simulated (a) input reflection coefficient S_{11} and (b) axial ratio AR of the proposed antenna for different I_s values.

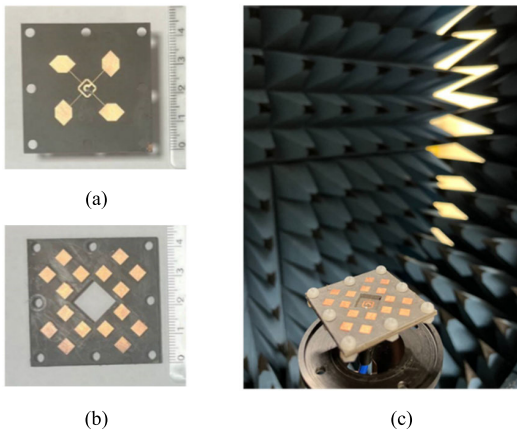


FIGURE 5. Constructed prototype of the proposed antenna: (a) top view of the substrate #1, (b) top view of the substrate #2, (c) assembled antenna in the Satimo StarLab anechoic chamber.

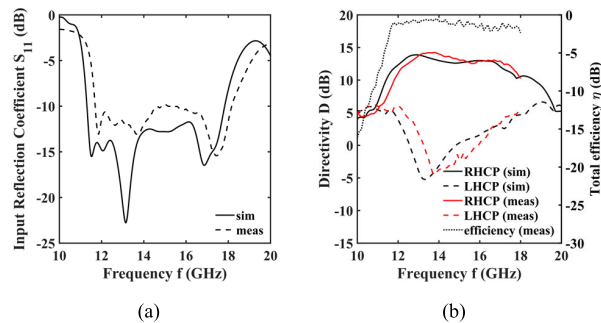


FIGURE 6. (a) Simulated (solid line) and measured (dashed line) input reflection coefficient S_{11} , (b) simulated (black line) and measured (red line) directivity D for RHCP (solid line) and LHCP (dashed line) radiation of the proposed antenna.

to i) fabrication tolerance; ii) not ideal stacking of the substrates, fixed with nylon screws; iii) connector soldering. Figure 6 (b) reports the simulated and measured directivity D for both RHCP radiation and left-hand circular polarization (LHCP) radiation as well as the measured total efficiency η .

The measured peak gain is $G = 13.9$ dBic with a 3 - dB gain bandwidth from $f = 12.3$ GHz to $f = 17.5$ GHz, i.e. a relative bandwidth of 34.9% within the impedance bandwidth. RHCP radiation (solid lines) is the dominant operating mode of the designed and fabricated antenna.

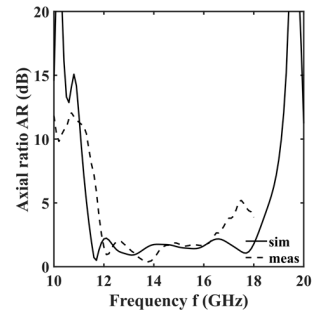
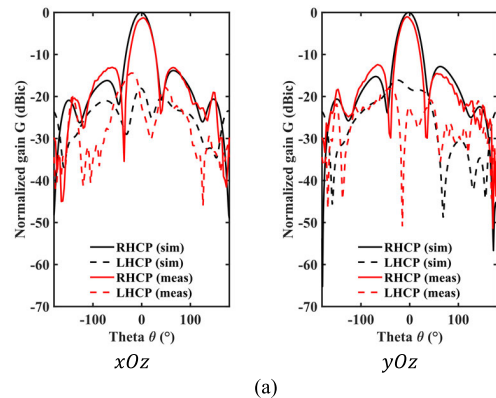
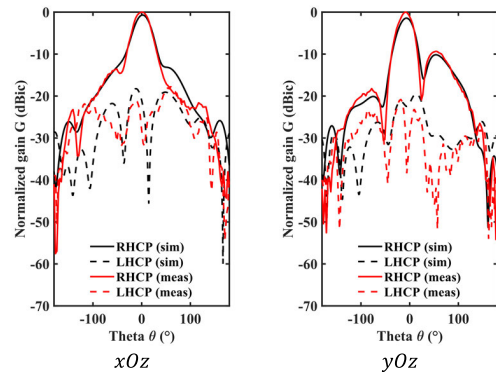


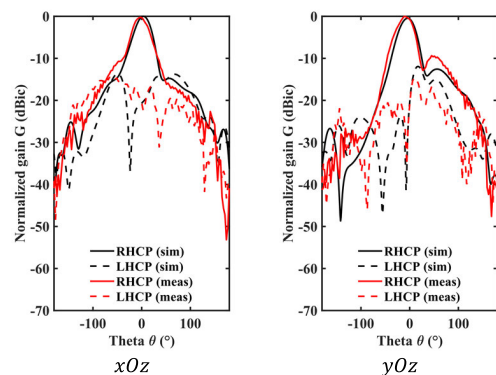
FIGURE 7. Simulated (solid line) and measured (dashed line) axial ratio AR of the proposed antenna.



(a)



(b)



(c)

FIGURE 8. Simulated (black line) and measured (red line) RHCP (solid line) and LHCP (dashed line) radiation patterns of the constructed antenna: a) frequency $f = 12$ GHz, b) frequency $f = 14$ GHz, c) frequency $f = 16$ GHz.

TABLE 2. Comparison with literature circularly polarized antennas.

Ref. no	Structure	Size (λ_0^3)	$S_{11} \leq -10dB$ (GHz)	$S_{11} \leq -10dB$ BW (%)	3 - dB AR BW (%)	3 - dB G BW (%)	Peak gain (dBic)	Number of substrates
[3]	Patch antenna array with stacked metasurface	1.26 × 1.26 × 0.046	4.4 ~ 8.0	55.6	41.7	18.2	12.1	2
[4]	Square ring, two layers patches and vertical walls	0.88 × 0.88 × 0.12*	4.7 ~ 7.2	43.2	26.5	32.6 **	8.5	2 + vertical walls
[14]	Sequential phase fed patch antenna array	1.55 × 1.55 × 0.03	5.2 ~ 6.2	18.7	12.7	12.7	12.0	1
[20]	Polarization conversion metasurface array	2.06 × 2.06 × 0.08*	5.4 ~ 7.5	32.6	26.35	—	13.5	2
[21]	SISL sequentially rotation feeding antenna	2.4 × 2.4 × 0.102*	5.0 ~ 6.2	20.2	18.9	> 20	13.8	5
[22]	3D M-Probe	1.39 × 1.39 × 0.14	10.8 ~ > 16	> 30.0	> 30.0	—	11.3	3
[23]	Rotated-stair dielectric resonator antenna	2.8 × 2.0 × 0.3*	10.1 ~ 13.0	25.1	21.4	—	15.1	3
This work	Sequential phase fed patch antenna array with holed metasurface	2.16 × 2.16 × 0.12	11.6 ~ 18.1	43.8	36.6	34.9	13.9	2

λ_0 is calculated as the free-space wavelength referring to the center frequency of the 3 - dB gain bandwidth

* λ_0 is calculated as the free-space wavelength referring to the center frequency of the impedance bandwidth

** 1 - dB gain bandwidth

The simulated and measured axial ratio AR is reported in Fig. 7, proving a measured 3 - dB axial ratio bandwidth from $f = 11.6$ GHz to $f = 16.8$ GHz (36.6%). The simulated 3 - dB AR bandwidth is larger than the measured one. This can be also ascribed to fabrication tolerance, presence of screws neglected in the simulation and connector soldering.

Figure 8 reports the antenna radiation patterns in the xOz and yOz planes at three different frequencies, (a) frequency $f = 12$ GHz, (b) frequency $f = 14$ GHz and (c) frequency $f = 16$ GHz. The RHCP radiation (solid lines), as expected, is the dominant operating mode of the designed and fabricated antenna.

The performance of the proposed antenna is compared to that of similar antenna designs in terms of antenna size, impedance bandwidth, 3 - dB AR bandwidth, 3 - dB gain bandwidth, peak gain, and fabrication complexity as shown in Table 2. By the table inspection, the proposed antenna has wide impedance matching, 3 - dB AR, and 3 - dB gain bandwidths. It is also worth mentioning that the proposed design operates at larger frequency and generated a peak gain of 13.9 dBic at the frequency $f = 14$ GHz. With respect to the state of the art, the proposed antenna exhibits an improvement in performance metrics while preserving a compact size with no air gaps.

IV. CONCLUSION

In this paper, a CP antenna designed for Ku-band applications is proposed. The antenna structure consists of a stacked configuration without air gaps, where a 2×2 square patch

metasurface array is placed directly above the sequential-phase fed patch antenna array.

The metasurface plays a key role in enhancing the antenna electromagnetic performance via surface wave propagation, introducing additional resonances to improve both the impedance bandwidth and the 3 - dB AR bandwidth.

The incorporation of a square-shaped aperture in the metasurface layer is demonstrated as novel effective approach to further enhance broadband performance, reducing phase delay variation among array elements over frequency in the sequential-phase feeding network. The designed and fabricated antenna predominantly operates in the right-hand circular polarization.

Experimental results demonstrate a high level of agreement with simulations, confirming the antenna performance in terms of impedance matching, stable gain, and broadband operation. Specifically, the antenna achieves a consistent gain above 10 dBic throughout the CP bandwidth, making it an ideal candidate for space-based applications, including satellite communications, and radar systems, where high gain, wide bandwidth, and reliable polarization performance are essential.

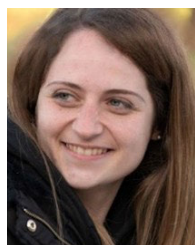
REFERENCES

- [1] S. X. Ta and I. Park, "Low-profile broadband circularly polarized patch antenna using metasurface," *IEEE Trans. Antennas Propag.*, vol. 63, no. 12, pp. 5929–5934, Dec. 2015, doi: 10.1109/TAP.2015.2487993.
- [2] W. Yang, J. Zhou, Z. Yu, and L. Li, "Single-fed low profile broadband circularly polarized stacked patch antenna," *IEEE Trans. Antennas Propag.*, vol. 62, no. 10, pp. 5406–5410, Oct. 2014, doi: 10.1109/TAP.2014.2344657.

- [3] S. X. Ta and I. Park, "Compact wideband circularly polarized patch antenna array using metasurface," *IEEE Antennas Wireless Propag. Lett.*, vol. 16, pp. 1932–1936, 2017, doi: [10.1109/LAWP.2017.2689161](https://doi.org/10.1109/LAWP.2017.2689161).
- [4] K. Ding, Y. Wu, K.-H. Wen, D.-L. Wu, and J.-F. Li, "A stacked patch antenna with broadband circular polarization and flat gains," *IEEE Access*, vol. 9, pp. 30275–30282, 2021, doi: [10.1109/ACCESS.2021.3059948](https://doi.org/10.1109/ACCESS.2021.3059948).
- [5] Nasimuddin, Z. N. Chen, and X. Qing, "Asymmetric-circular shaped slotted microstrip antennas for circular polarization and RFID applications," *IEEE Trans. Antennas Propag.*, vol. 58, no. 12, pp. 3821–3828, Dec. 2010, doi: [10.1109/TAP.2010.2078476](https://doi.org/10.1109/TAP.2010.2078476).
- [6] J. M. Kovitz and Y. Rahmat-Samii, "Using thick substrates and capacitive probe compensation to enhance the bandwidth of traditional CP patch antennas," *IEEE Trans. Antennas Propag.*, vol. 62, no. 10, pp. 4970–4979, Oct. 2014, doi: [10.1109/TAP.2014.2343239](https://doi.org/10.1109/TAP.2014.2343239).
- [7] Q. W. Lin, H. Wong, X. Y. Zhang, and H. W. Lai, "Printed meandering probe-fed circularly polarized patch antenna with wide bandwidth," *IEEE Antennas Wireless Propag. Lett.*, vol. 13, pp. 654–657, 2014, doi: [10.1109/LAWP.2014.2314141](https://doi.org/10.1109/LAWP.2014.2314141).
- [8] N. Hussain, M.-J. Jeong, J. Park, and N. Kim, "A broadband circularly polarized Fabry–Pérot resonant antenna using a single-layered PRS for 5G MIMO applications," *IEEE Access*, vol. 7, pp. 42897–42907, 2019, doi: [10.1109/ACCESS.2019.2908441](https://doi.org/10.1109/ACCESS.2019.2908441).
- [9] N. Nguyen-Trong, H. H. Tran, T. K. Nguyen, and A. M. Abbosh, "A compact wideband circular polarized Fabry–Pérot antenna using resonance structure of thin dielectric slabs," *IEEE Access*, vol. 6, pp. 56333–56339, 2018, doi: [10.1109/ACCESS.2018.2872571](https://doi.org/10.1109/ACCESS.2018.2872571).
- [10] Y. Liu, K. Song, Y. Qi, S. Gu, and X. Zhao, "Investigation of circularly polarized patch antenna with chiral metamaterial," *IEEE Antennas Wireless Propag. Lett.*, vol. 12, pp. 1359–1362, 2013, doi: [10.1109/LAWP.2013.2286191](https://doi.org/10.1109/LAWP.2013.2286191).
- [11] S.-K. Lin and Y.-C. Lin, "A compact sequential-phase feed using uniform transmission lines for circularly polarized sequential-rotation arrays," *IEEE Trans. Antennas Propag.*, vol. 59, no. 7, pp. 2721–2724, Jul. 2011, doi: [10.1109/TAP.2011.2152346](https://doi.org/10.1109/TAP.2011.2152346).
- [12] K. Ding, C. Gao, D. Qu, and Q. Yin, "Compact broadband circularly polarized antenna with parasitic patches," *IEEE Trans. Antennas Propag.*, vol. 65, no. 9, pp. 4854–4857, Sep. 2017, doi: [10.1109/TAP.2017.2723938](https://doi.org/10.1109/TAP.2017.2723938).
- [13] K. L. Chung, S. Chaimool, and C. Zhang, "Wideband subwavelength-profile circularly polarised array antenna using anisotropic metasurface," *Electron. Lett.*, vol. 51, no. 18, pp. 1403–1405, Sep. 2015, doi: [10.1049/el.2015.2255](https://doi.org/10.1049/el.2015.2255).
- [14] C. Deng, Y. Li, Z. Zhang, and Z. Feng, "A wideband sequential-phase fed circularly polarized patch array," *IEEE Trans. Antennas Propag.*, vol. 62, no. 7, pp. 3890–3893, Jul. 2014, doi: [10.1109/TAP.2014.2321380](https://doi.org/10.1109/TAP.2014.2321380).
- [15] F. Costa, O. Luukkonen, C. R. Simovski, A. Monorchio, S. A. Tretyakov, and P. M. de Maagt, "TE surface wave resonances on high-impedance surface based antennas: Analysis and modeling," *IEEE Trans. Antennas Propag.*, vol. 59, no. 10, pp. 3588–3596, Oct. 2011, doi: [10.1109/TAP.2011.2163750](https://doi.org/10.1109/TAP.2011.2163750).
- [16] K. Agarwal, Nasimuddin, and A. Alphones, "Wideband circularly polarized AMC reflector backed aperture antenna," *IEEE Trans. Antennas Propag.*, vol. 61, no. 3, pp. 1456–1461, Mar. 2013, doi: [10.1109/TAP.2012.2227446](https://doi.org/10.1109/TAP.2012.2227446).
- [17] N. Hussain, M.-J. Jeong, A. Abbas, T.-J. Kim, and N. Kim, "A metasurface-based low-profile wideband circularly polarized patch antenna for 5G millimeter-wave systems," *IEEE Access*, vol. 8, pp. 22127–22135, 2020, doi: [10.1109/ACCESS.2020.2969964](https://doi.org/10.1109/ACCESS.2020.2969964).
- [18] S. X. Ta and I. Park, "Artificial magnetic conductor-based circularly polarized crossed-dipole antennas: 1. AMC structure with grounding pins: AMC-BASED CP CROSSED-DIPOLE ANTENNA: 1," *Radio Sci.*, vol. 52, no. 5, pp. 630–641, May 2017, doi: [10.1002/2016rs006203](https://doi.org/10.1002/2016rs006203).
- [19] M. Fereidani Samani and R. Safian, "On bandwidth limitation and operating frequency in artificial magnetic conductors," *IEEE Antennas Wireless Propag. Lett.*, vol. 9, pp. 228–231, 2010, doi: [10.1109/LAWP.2010.2046390](https://doi.org/10.1109/LAWP.2010.2046390).
- [20] W. Zhang, Y. Liu, and Y. Jia, "Circularly polarized antenna array with low RCS using metasurface-inspired antenna units," *IEEE Antennas Wireless Propag. Lett.*, vol. 18, pp. 1453–1457, 2019, doi: [10.1109/LAWP.2019.2919716](https://doi.org/10.1109/LAWP.2019.2919716).
- [21] N. Yan, K. Ma, and Y. Luo, "An SISL sequentially rotated feeding circularly polarized stacked patch antenna array," *IEEE Trans. Antennas Propag.*, vol. 68, no. 3, pp. 2060–2067, Mar. 2020, doi: [10.1109/TAP.2019.2957096](https://doi.org/10.1109/TAP.2019.2957096).
- [22] H. W. Lai, D. Xue, H. Wong, K. K. So, and X. Y. Zhang, "Broadband circularly polarized patch antenna arrays with multiple-layers structure," *IEEE Antennas Wireless Propag. Lett.*, vol. 16, pp. 525–528, 2017, doi: [10.1109/LAWP.2016.2587302](https://doi.org/10.1109/LAWP.2016.2587302).
- [23] W.-W. Yang, W.-J. Sun, H. Tang, and J.-X. Chen, "Design of a circularly polarized dielectric resonator antenna with wide bandwidth and low axial ratio values," *IEEE Trans. Antennas Propag.*, vol. AP-67, no. 3, pp. 1963–1968, Mar. 2019, doi: [10.1109/TAP.2019.2891219](https://doi.org/10.1109/TAP.2019.2891219).



FRANCESCO ANELLI received the B.Sc. degree (cum laude) in electronic and telecommunication engineering, the M.Sc. degree (cum laude) in electronic engineering, and the Ph.D. degree (cum laude) in information and electrical engineering from the Politecnico di Bari, Italy, in 2019, 2021, and 2024, respectively. He is currently a Non-Tenured Assistant Professor with the Politecnico di Bari. His research interests include the design, fabrication, and characterization of metasurface-based antennae and optical fiber components for mid-infrared applications.



ANTONELLA MARIA LOCONSOLE received the Ph.D. degree in electrical and information engineering from the Politecnico di Bari, Bari, Italy, in 2022. She is currently a Research Assistant in electromagnetic fields with the Department of Electrical and Information Engineering, Politecnico di Bari. Her research interests include SIW antennas, microwave applicators for medical applications, and optical fiber lasers and amplifiers.



RICCARDO LOSITO received the master's degree (Hons.) in medical systems engineering from the Politecnico di Bari, Italy, in 2024. His research interests include the design and development of broadband microstrip antennas, as well as the study and application of metamaterials and metasurfaces.



FRANCESCO PRUDENIANO (Member, IEEE) received the Ph.D. degree in electronic engineering from the Politecnico di Bari, Bari, Italy, in November 1996. Since 2018, he has been a Full Professor of electromagnetic fields with the Department of Electrical and Information Engineering, Politecnico di Bari. Since October 2024, he has been the Head of the Department of Electrical and Information Engineering, Politecnico di Bari. He is currently the Head of the Microwave and Optical Engineering Group, Department of Electrical and Information Engineering, Politecnico di Bari. He is involved in several national and international research projects and cooperations. He has co-authored more than 410 publications, 300 of which were published in journals and international conferences, lectures, and invited papers. His research interests include the design and characterization of microwave devices, integrated optics, and optical fiber-based devices. From 2017 to 2018, he was the Chair of SIOF, the Italian Society of Optics and Photonics (Italian Branch of EOS—the European Optical Society).